



# Environmental cues in different host niches shape the survival fitness of *Staphylococcus aureus*

Received: 16 August 2024

Accepted: 17 July 2025

Published online: 28 July 2025

JuOae Chang<sup>1,6</sup>, ChaeYoung Lee<sup>1,6</sup>, Inseo Kim<sup>1</sup>, Jihyeon Kim<sup>1</sup>, Ji-Hoon Kim<sup>1</sup>, Taegwan Yun<sup>1,2</sup>, David C. Hooper<sup>3</sup>, Suzanne Walker<sup>4,5</sup>  & Wonsik Lee<sup>1</sup> 

The ability of *Staphylococcus aureus* to adapt and thrive in diverse host niches adds to the challenge in combating this ubiquitous pathogen. While extensive research has been pursued on the adaptive mechanisms of methicillin-resistant *S. aureus* (MRSA) in various infection models, a comprehensive analysis of its fitness across different host niches is lacking. In this study, we employ transposon sequencing to analyze the adaptive strategies of MRSA in various infection niches. Our analysis encompasses a cell model that mimics an intracellular niche, human blood, which represents a major extracellular environment as well as a major intermediary route encountered by bacteria during systemic infection, and a male murine sepsis model that recapitulates intra-organ environments. Our findings reveal substantial differences in the genetic determinants essential for bacterial survival in intracellular and blood environments. Moreover, we show that each organ imposes unique growth constraints, thus fostering heterogeneity within the mutant population that can enter and survive in each organ of the mouse. By comparing genes important for survival across all examined host environments, we identify 27 core genes that represent potential therapeutic targets for treating *S. aureus* infections. Additionally, our findings aid in understanding how bacteria adapt to diverse host environments.

Bacteremia caused by methicillin-resistant *Staphylococcus aureus* (MRSA) is a leading cause of human death resulting from bacterial infections, posing a serious threat to public health<sup>1–3</sup>. However, treatment of MRSA infection has been hampered not only by the continual emergence of evolved MRSA strains but also by the acquisition of mechanisms to invade and survive in the intracellular niches of host cells<sup>4–6</sup>. Therefore, identification of the underlying networks and genes required for the intracellular entry and survival of *S. aureus* can provide essential information for the development of antibacterial therapies.

*S. aureus* is commonly found as a commensal in different body parts of the human host, but exposure to different niches and conditions can transform it into a devastating pathogen that causes permanent organ damage or death<sup>7,8</sup>. Previously classified as a strictly extracellular pathogen, *S. aureus* is now also considered to be able to establish an intracellular infection<sup>4–6,9</sup>. It begins its infection by colonizing various host surfaces and matrices and establishing extracellular infections. Then, it can proliferate and reach the bloodstream of the host and further penetrate major organs such as the liver and lungs; while traveling around the bloodstream, *S. aureus* can also reach

<sup>1</sup>School of Pharmacy, Sungkyunkwan University, Suwon, Republic of Korea. <sup>2</sup>Department of Biopharmaceutical Convergence, Sungkyunkwan University, Suwon, Republic of Korea. <sup>3</sup>Division of Infectious Diseases, Massachusetts General Hospital, Harvard Medical School, Boston, MA, USA. <sup>4</sup>Department of Microbiology, Harvard Medical School, Boston, MA, USA. <sup>5</sup>Department of Chemistry and Chemical Biology, Harvard University, Cambridge, MA, USA. <sup>6</sup>These authors contributed equally: JuOae Chang, ChaeYoung Lee. ✉e-mail: [suzanne\\_walker@hms.harvard.edu](mailto:suzanne_walker@hms.harvard.edu); [wonsik.lee@skku.edu](mailto:wonsik.lee@skku.edu)

intracellular niches to establish infection. To switch to its pathogenic mode in all these different host niches, *S. aureus* relies on a fine-tuned network of transcription factors and two-component systems (TCSs). These regulatory systems not only control its ability to adapt to different nutrient environments and cope with different levels of oxidative stress, but also facilitate activation of protective mechanisms, such as biofilm formation, which contribute to its virulence and survival in the host<sup>10,11</sup>. The ability of *S. aureus* to switch rapidly from living extracellularly to living intracellularly is also attributed to its metabolic and physiological plasticity, which is controlled by these numerous regulators. Among these regulators, Agr, SaeRS, and the recently discovered SrrAB are thought to be hubs of the regulatory circuitry for *S. aureus* survival in the host<sup>10,12,13</sup>. For example, SaeRS governs key reprogramming during infection by signaling for the induction of stress response molecules, cation transporters, and membrane remodeling proteins<sup>14,15</sup>. These mechanisms of regulation for survival represent potential druggable targets to antagonize MRSA persistence and improve clinical outcomes.

The plasticity of the metabolic and regulatory circuits of *S. aureus* allows it to efficiently establish infections in almost any niche, whether extracellular, intracellular, or body organ, and renders it capable of quickly switching between niches. Over the past decades, mechanisms governing in vivo infection or intracellular survival of *S. aureus* have been extensively studied using transcriptomic and genetic profiling<sup>16–19</sup>. However, results obtained from one infection model may not necessarily apply to another. To address the need for a comprehensive analysis of adaptive mechanisms required for *S. aureus* survival in various niches, we investigate in this study how the fitness of *S. aureus* transposon mutants changes in different niches. We performed transposon sequencing (Tn-seq) on a pooled *S. aureus* mutant library using a cell infection model that recapitulates an intracellular niche, human blood that represents an extracellular niche as well as a major intermediary route for *S. aureus* to reach the organs, and a mouse sepsis model to show adaptation mechanisms in major organs involved in infection. We find that most genes and regulons required for intracellular infection are distinct from those required for survival in an extracellular environment. The results from the in vivo sepsis model bear strong similarities to the results for human blood, suggesting that *S. aureus* is primarily exposed to the extracellular rather than the intracellular environment during sepsis. However, from the sepsis model, we also found that the environment of each organ imposes different constraints on the growth of *S. aureus*, uniquely shaping the *S. aureus* population within each organ. Our results suggest that targeting genes essential during infection may combat *S. aureus* infection and the progression of sepsis, and we describe a core set of genes important for infection in all environments that may be particularly effective therapeutic targets.

## Results

### Transposon sequencing reveals genetic remodeling important for *S. aureus* survival in intracellular infection

First, we established a cell infection model using a *S. aureus* transposon (Tn) mutant library and analyzed the genes required for the early and late phases of intracellular infection (Fig. 1a). We wanted a minimal bottleneck effect for our genetic analysis, so we first assessed an infection efficiency of the methicillin-resistant *S. aureus* (MRSA) strain USA300 in three cell lines relevant to *S. aureus* infection. A549 cells derived from the lungs allowed entry of almost all bacterial cells, while 50% and less than 10% of the bacteria entered murine macrophage (Raw264.7) cells and human keratinocyte (HaCaT) cells, respectively (Fig. 1b). Based on the finding that A549 cells are permissive to bacterial infection and survival compared to the other cell lines, we selected this cell line for our model. We next examined whether A549 cells are permissive to the entry of several other MRSA strains or methicillin-sensitive *S. aureus* (MSSA) strains. The MRSA strains

USA300 and MW2 demonstrated the highest infection rates, whereas MSSA strain Newman was non-invasive (Fig. 1c). These results show that there can be very large differences in cell infection efficiency among different pathogenic *S. aureus* strains<sup>20</sup>. We selected USA300 for genetic profiling because it represents the predominant community-acquired MRSA clone in North America and is therefore of high current interest<sup>21,22</sup>. We found that USA300 is not only able to efficiently invade A549 cells but also proliferates intracellularly up to 8 h post-infection (Fig. 1d), consistent with previous observations<sup>5,23</sup>. Interestingly, we did not observe proliferation for the MSSA strain HG003, which is in the same clonal complex as USA300 (Supplementary Fig. 1), showing that USA300 is better adapted for intracellular growth. To confirm that USA300 cells indeed grow and divide intracellularly, we examined infected A549 cells using transmission electron microscopy (Fig. 1e). At 4 h post-infection, we observed multiple *S. aureus* cells with septa, indicating that these bacteria were in the process of division inside the host cells when the samples were processed. Growth and division in the intracellular environment were also confirmed by fluorescence microscopy using a USA300 strain expressing FtsZ-GFP (Fig. 1f).

We next infected the A549 cells with a USA300 Tn mutant library at a multiplicity of infection (MOI) of 10, which resulted in full recovery of input bacteria. The mutant library used in this study is a high-density library containing more than 760,000 Tn mutants made by phage-based transposition<sup>24</sup>. The number of mutants exceeds the number of TA sites in the *S. aureus* genome because the library is composed of six bar-coded sublibraries, each produced using a slightly different Tn construct. Some constructs have outward-facing promoters that can minimize the polar effects of insertion on downstream gene expression. Tn mutants recovered right after infection (at 0 h post-infection) were used to identify genes required for the early stage of infection, while Tn mutants recovered at 2, 4, and 8 h post-infection were analyzed to identify genes required for intracellular proliferation (Fig. 1a). A Tn library not exposed to the host cells was used as an input control. After sequencing, the read counts due to the Tn insertions for each gene were mapped to the genome of USA300, generating a complete profile for all time points. The percentage of TA sites containing the Tn insertions was comparable to the input at each time point, suggesting a minimal bottleneck effect (Fig. 1g, table). Moreover, Circos plots of the read counts for each TA site confirm high coverage of Tn mutants across the genome (Fig. 1g and Supplementary Fig. 2, green bars). In these plots, genes for which reads were depleted and enriched compared with the input control are represented in blue and orange (Fig. 1g, magnification), respectively. Among the genes required for intracellular survival (depleted reads compared with the input control), we found SaeRS, a TCS previously shown to be required during host invasion (Fig. 1h), which validates our genetic analysis<sup>25</sup>.

### *S. aureus* faces nutrient limitation during intracellular infection

Since we aimed to identify genes required for intracellular infection, we focused on only the depleted genes in the Tn-seq analysis. For this, we plotted the read counts of the genes from each sample against those of the input and set up a significance cut-off as 1.3-fold decrease of log<sub>2</sub> fold change with a *P* value ≤ 0.05 (Fig. 2a). We have excluded the genes with a small read count (<50) in the control input library from our further analysis as done in previous studies<sup>26,27</sup>. Based on our Tn-seq datasets, we categorized genes as early or late essential based on changes of read counts during an 8-h infection period. A total of 226 genes were identified as essential for intracellular infection from the early stages to the proliferation (late) stages; 11 genes were categorized as early essential, 44 genes as essential for proliferation (late essential), and 72 genes essential for both the early and proliferation stages (Fig. 2b). Genes that were substantially changed and clustered were represented as a heat map (Fig. 2c) with a complete list provided in Supplementary Fig. 3. Importantly, as marked by the black lines above

the genes in Fig. 2c, multiple genes belonging to the same functional group are consistently depleted, thereby providing cross-validation for their functional importance.

In Fig. 3a, we summarized the sets of genes required for the intracellular infection, which include genes involved in cell wall biogenesis (*murA*, *mprF*, and *pgcA*), pathogenesis (*sae*, *mra* and *nre* loci), nutrient/ion uptake (i.e., *mnh*, *mpf* and *sir* loci), stress response (i.e., *clpC* and *ahpF*), energy production (i.e., *atp* and *pur* loci), and carbon source utilization (i.e., *citB* and *dap* locus). We also included a full list of genes required at each stage of infection by listing all genes that appeared to be required at least at one time point during the infection period (Supplementary Fig. 3). Among these genes, the greatest depletion across all time points was observed in *saeS* and *saeR*. The SaeRS TCS responds to host environmental cues (i.e., calprotectin, oxidative stress, and neutrophil proteins) and relays signals to produce virulence factors for adhesion, proteolysis, and hemolysis (i.e., *hla*)<sup>28</sup>. Therefore, SaeRS plays a central role in adaptation to the host milieu. Additionally, we identified other transcriptional regulators, *nre* and *mra* loci, as essential for intracellular survival. However, we did not observe *srrA*, which is involved in responding to nitric oxide stress, perhaps because A549 is an epithelial cell line with weak phagocytic

activity<sup>29</sup>. Interestingly, we found groups of genes for which the extent of depletion was not consistent throughout the sampling time points (included in the last category in Supplementary Fig. 3). Among these, *murA* was depleted at 0 and 4 h but not at 2 and 8 h (Fig. 2c). In addition, menaquinone (MQ) biosynthesis genes such as *men* and *aro* loci were substantially depleted in read counts during the early stage rather than the late stages therefore classified as early essential. MQ is electron-charged between ATP synthase and cytochrome oxidase in the ATP generation system of *S. aureus*<sup>30,31</sup>. When we analyzed the whole locus of the *men* operon, most genes were depleted, suggesting a requirement for MQ during the early stage of infection. To validate genes involved in this early stage, we tested individual mutants with the Tn insertion in the identified genes. Mutants of the genes found to be involved in the early phase of infection (i.e., *aroB* or *menD*) invaded less into the host cells than the wild-type strain, as shown in Fig. 3b. Although mutants with the Tn insertion at these genes grow slowly (Supplementary Fig. 4a), we do not think slow growth explains these early phase results because other mutants with growth defects did not appear in our Tn-seq results.

Along with the early essential group of genes, we found another group of genes that were depleted to a greater degree during the late

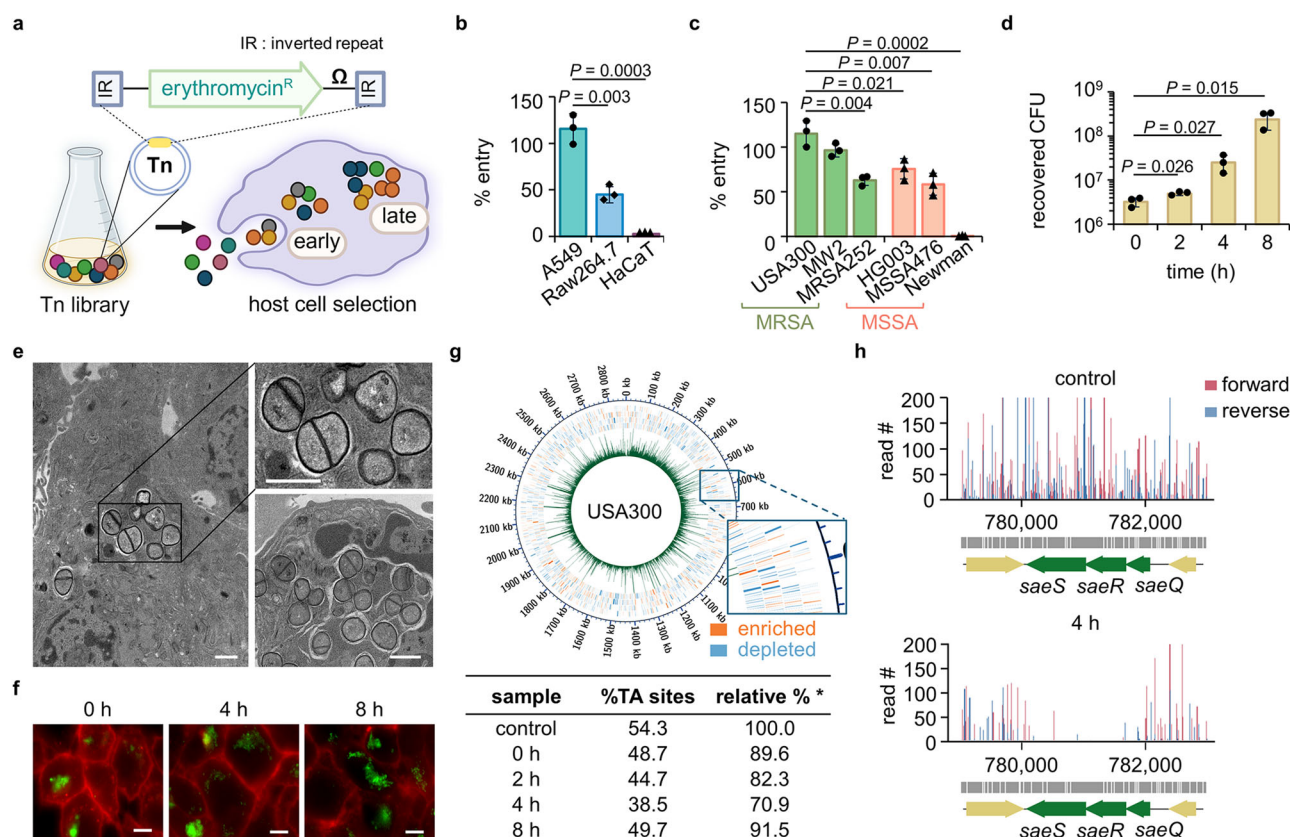


**Fig. 1 | Methicillin-resistant *S. aureus* USA300 establishes infection in mammalian cells.** **a** To determine genes essential for the early entry into and late survival in host cells, A549 cells were infected with the USA300 Tn library for 1.5 h, after which extracellular bacteria were removed by gentamicin. Samples collected right after gentamicin were defined as 0 h throughout the manuscript. Image created in BioRender (Lee, W. (2025) <https://BioRender.com/bytpvde>). Extent of infection (**b**) of USA300 into host cells (A549, Raw264.7, and HaCat) and (**c**) of MRSA and MSSA strains into A549 cells were determined by cell infection assay (% entry =  $\frac{\text{CFU recovered at 0 h}}{\text{input CFU}} \times 100$ ). **d** The CFU were counted at 0–8 h post-infection as a measure of USA300 survival inside the A549 cells. Data in **b–d** are presented as the mean  $\pm$  SD ( $n = 3$  biological replicates);  $P$  values are calculated by a two-sided, unpaired Student's  $t$ -test. Source data for **b–d** are available in the **Source Data** file. **e** The intracellular bacteria were examined by transmission electron microscopy at

4 h post-infection (scale bar = 1  $\mu$ m). **f** Entry and survival of FtsZ-GFP-expressing USA300 in A549 cells were inspected by fluorescence microscopy. The cell membrane and bacteria are shown in red and green, respectively (scale bar = 5  $\mu$ m). The images in **e–f** are representative of three independent experiments. **g** The entire sequenced genome at 0 h was plotted using Circos with the green peaks representing read counts for each TA site and blue and orange outer squares representing genes with counts lower (depleted) and higher (enriched) than those of the control library, respectively. The % TA sites (% TA sites detected out of all TA sites in the genome) show the coverage of the genome by Tn-seq and are presented in a table (\* relative % =  $\frac{\% \text{TA sites of an experimental sample}}{\% \text{TA sites of a control Tn library (54.3\%)}} \times 100$ ). **h** The read counts generated by sequencing in both forward (red) and reverse (blue) directions for each TA site within the *saeQRS* locus of the control and 4 h samples were plotted using R.



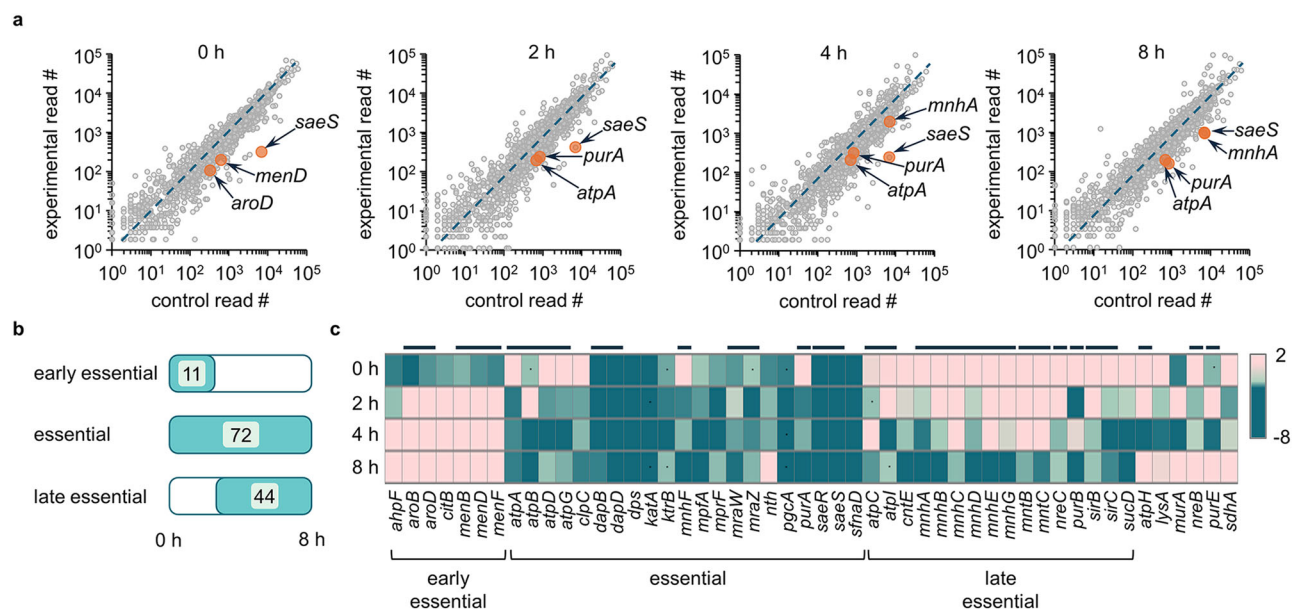


**Fig. 2 | Tn-seq reveals several genes essential for intracellular entry and post-entry survival of methicillin-resistant *S. aureus*.** **a** Read counts from samples collected at 0 h and during intracellular survival (2–8 h post-infection) were plotted against the read counts of the respective genes of the control (not exposed to host cells) sample. The *saeS* gene is represented on the graphs as a gene depleted at all time points, while *menD* and *aroD* are representative genes depleted at an earlier stage of infection. Genes, such as *purA*, *atpA*, and *mnhA*, represent genes that appear later during the intracellular infection. Source data is available in the **Source Data** file. **b** Genes that demonstrated a substantial decrease in their read counts ( $\log_2$  fold change  $\leq -1.3$ ,  $P$  value  $\leq 0.05$ ) were classified into genes that are entry-specific (early essential; substantially depleted at 0–2 h post-infection), common

for entry and post-entry events (essential; substantially depleted at 3 or more time points throughout the experiment (0–8 h)), or post-entry survival-specific (late essential; depleted only at 8 h, 2 + 8 h, or 4 + 8 h post-infection). The numbers of genes in each category are presented in a table. **c** Representative early essential and late essential genes, and genes essential throughout the infection period are expressed as a heat map. The heat map also includes representative genes that are depleted at one or two time points but do not fall into any of the classification categories. Genes were considered essential if  $\log_2$  fold change  $\leq -1.3$  with  $P$  value  $\leq 0.05$ ; dots on the heat map present genes that meet the  $\log_2$  fold change criterion but not the  $P$  value criterion, and the black lines above the heat map express genes appearing in a gene group.

stage of infection or were depleted throughout the 8-h period. These include genes involved in ATP generation (*atp* and *pur* loci) and multiple genes related to nutrient uptake: transmembrane transporters (i.e., *cntE* and *mnh* locus) that transport metals and ions across the membrane and iron acquisition genes (i.e., *sir* locus and *sfnA*) involved in siderophores or iron acquisition. Finally, we also identified genes related to the oxidative stress response (i.e., *nth* and *kata*) and general stress response (i.e., *clpC*) to be essential for survival in the intracellular milieu (Fig. 3a). These results suggest that intracellular *S. aureus* faces a severe limitation of nutrients, including essential metal ions. In addition, the essentiality of genes involved in the TCA cycle (i.e., *citB* and *sucD*) suggests that *S. aureus* may become heavily dependent on the TCA cycle and electron transport chain (ETC) to produce ATP, since substrate-level ATP production via glycolysis might become limited due to the limited availability of glucose or other hexose sugar sources while non-carbohydrate carbon sources such as lactate or fatty acid may be more available in the intracellular environment of the host cell. To validate these genes, we chose key genes in each pathway, and mutants of these genes showed no detectable growth defects in TSB medium (Supplementary Fig. 4b) but low fitness when tested individually in the A549 infection assay (Fig. 3c and Supplementary Fig. 4c). Also, the operon analysis showed that many genes required for intracellular invasion and survival were included within the same operon, further validating our Tn-seq analysis (Supplementary Fig. 5). Since we found multiple genes for the ETC including MQ biosynthesis genes, *atpA* and *sucD*, we wanted to validate the essentiality of ATP generation via the ETC by testing bacterial survival in A549 cells in the presence of oligomycin A, a macroide that inhibits the F1F0-ATPase complex by binding to the F0 subunits 6 and 9<sup>32</sup>. As shown in Fig. 3d, at a concentration that affects neither bacteria

nor the host A549 cells (Supplementary Fig. 6a–b), bacteria exposed to an ATPase inhibitor demonstrated reduced infection and survival in the intracellular environment.

### ***S. aureus* extracellular proliferation in human blood requires different genes from those required for intracellular survival**

Invasive *S. aureus* infections result when *S. aureus* forms colonies on vulnerable bodily surfaces such as abraded skin and somehow reaches the circulatory system, causing bacteremia<sup>33</sup>. Since blood is considered a major extracellular environment for bacteria during systemic infection, we aimed to understand the physiological and metabolic changes that occur in *S. aureus* during bacteremia by identifying genes essential for survival in whole blood and plasma using the USA300 Tn library (Fig. 4a). The human blood used in this study was commercially sourced and treated with heparin, so the immune cells are likely mostly deactivated. Utilizing this system, we aimed to study the fitness of mutants in the blood as a host environment with a distinct set of nutrients and carbon sources without rapid clearance by immune cells. We first monitored the growth of USA300 in both human whole blood and plasma by measuring colony forming units (CFU) over 36 h. We found that in both whole blood and plasma, the CFU of USA300 reached a plateau at 9 h (Fig. 4b and Supplementary Fig. 7a), which is comparable to the growth profile in the TSB medium (Supplementary Fig. 4a–b). We used electron microscopy to examine whether the majority of USA300 remained outside of red blood cells (RBC) and found only minor infiltration of USA300 into RBC (Supplementary Fig. 7b).

For Tn-seq analysis, we collected *S. aureus* cells at 24 or 36 h based on the growth profile (Fig. 4b and Supplementary Fig. 7a). This allowed *S. aureus* to grow for over 10 generations, enabling sufficient time for

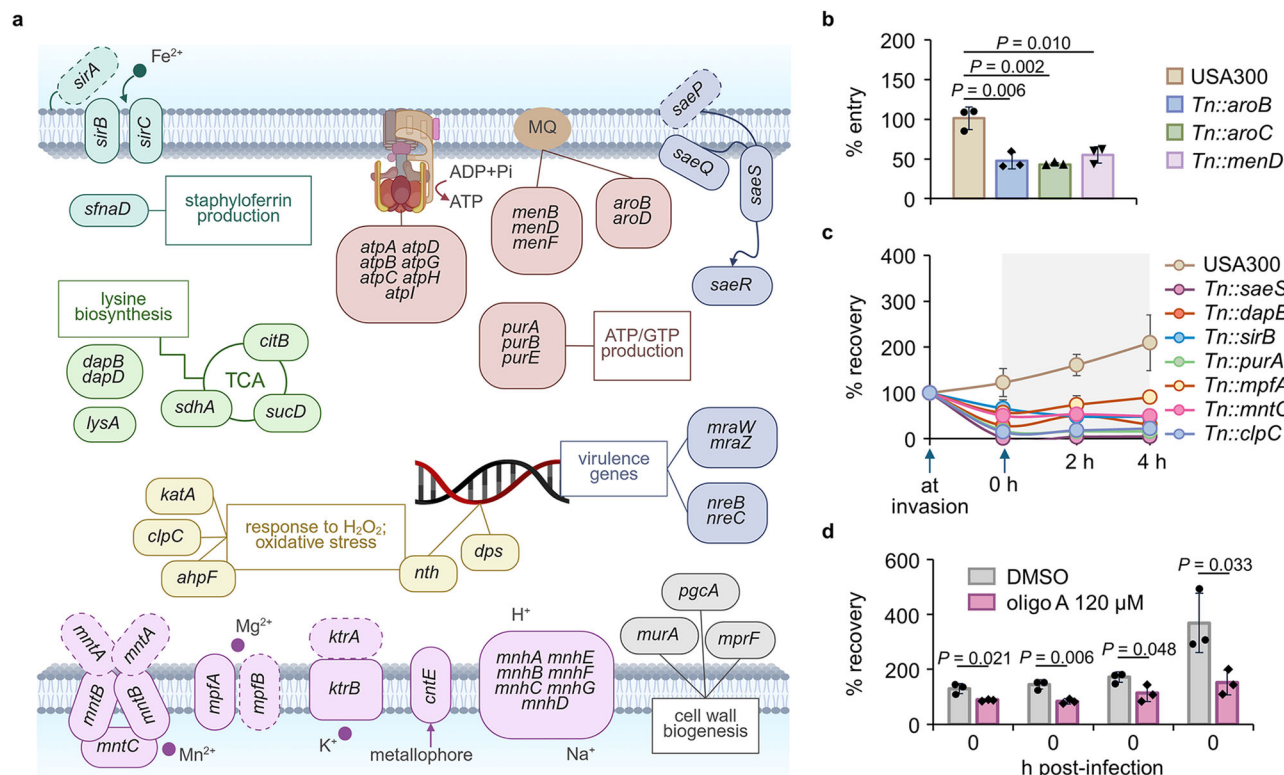


**Fig. 3 | Genes responsible for entry into and survival in host cells are grouped into functional groups. a** The genes involved in intracellular survival are grouped by their functions, and the selected pathways are presented in a diagram. Genes that were not substantially depleted but are needed as part of the functional group are marked with dotted lines. MQ, menaquinone. Image created in BioRender (Lee, W. (2025) <https://BioRender.com/sfrjhgvy>). The mutants of selected genes were obtained from the Nebraska Tn library and were confirmed for their role in **(b)** intracellular entry or **(c)** both entry and post-entry survival by the infection assay

(% entry =  $\frac{\text{CFU recovered at 0 h}}{\text{input CFU}} \times 100$ ; % recovery =  $\frac{\text{CFU recovered from cells}}{\text{input CFU}} \times 100$ ). **d** USA300 pre-exposed to 120  $\mu\text{M}$  of oligomycin A (oligo A), an ATPase inhibitor, was examined for the extent of infection into and proliferation inside the host A549 cells in the presence of 120  $\mu\text{M}$  oligomycin A (% recovery =  $\frac{\text{CFU recovered from cells}}{\text{input CFU}} \times 100$ ). Data in **b–d** are presented as the mean  $\pm$  SD ( $n = 3$  biological replicates), and the  $P$  values are calculated by a two-sided, unpaired Student's  $t$ -test. The source data for **b–d** are available in the **Source data** file.

identification of mutants with lower fitness. We first plotted the read counts from the Tn library cultured in whole blood or plasma against those from TSB media (Fig. 4c and Supplementary Fig. 8a). Primarily, we focused on the depleted genes. A total of 115 genes were found to be essential for survival in the blood ( $\log_2$  fold change  $\leq -1.2$ ;  $P$  value  $\leq 0.05$ ), and we found no notable differences between genes essential for survival in plasma and those essential for survival in whole blood (Supplementary Fig. 8b). Representative depleted genes are displayed in Fig. 4d. Among these were genes related to metal ion uptake (i.e., *isd*, *mnh*, and *mnt* loci), stress response (i.e., *yjb* locus, *clpC*, and *trxB*), and ATP metabolism (i.e., *atp* and *qox* loci). We further compared the depleted genes with those depleted during intracellular infection. We identified distinct genes essential for each growth condition and classified them into seven major functional groups (Fig. 4e). We found that genes encoding major TCSs of *S. aureus*, including *saeRS*, *agrD*, *sarR*, *srrA*, and *mgrA*, are differentially required in the two environments: *saeRS* is required for intracellular survival, while *srrA* is necessary for survival in blood, suggesting that different groups of TCSs are required for survival in these two environments. Genes related to oxidative stress responses, such as *perR* and *hslU*, were identified only in the blood conditions, suggesting that *S. aureus* may face more oxidative stress in the bloodstream compared to the intracellular environment of non-phagocytic cells. However, genes responsible for ATP production (i.e., *pur* and *atp* loci) and ion/metal balance (i.e., *mnh* and *mnt* loci) were depleted in both conditions, suggesting that in both conditions, *S. aureus* may be exposed to limited nutrients and an environment where ATP is primarily produced through the

electron transport chain. Similar to the results from the intracellular invasion, the operon analysis further confirmed that many genes required for survival in blood were within the same operon (Supplementary Fig. 9).

To validate our Tn-seq results, we selected mutants from the seven functional groups and tested them for their growth in blood. As shown in Fig. 4f, these mutants showed lowered fitness in blood. Importantly, we were able to confirm the Tn-seq result for *saeS* and *saeR*; as shown in Fig. 4g, we found no growth phenotype of these mutants in blood, suggesting that *S. aureus* regulates genes independently of SaeRS in blood. Regarding genes related to ATP production, we were also able to validate their requirement using oligomycin A. As shown in Fig. 4h, in the presence of oligomycin A, the growth of USA300 was delayed. Finally, we note that we observed no growth defects of the tested mutants in TSB medium, suggesting that the reduced fitness in blood is not due to the inactivated genes (Supplementary Fig. 4b and 10). Additionally, since the *mnh* operon appeared to be essential for survival in human blood, we generated  $\Delta mnhF$  for validation of its essentiality for blood survival. Although the *mnhF* mutant demonstrated growth defects compared to wild type (Supplementary Fig. 11a), the extent of reduced blood survival within 48 h surpasses the growth retardation (Supplementary Fig. 11b), implying that the reduced fitness is not simply due to slow growth caused by gene inactivation. In addition, the time-dependent decrease in the read counts of the genes provides validation for the essentiality of these genes for blood survival (Fig. 4i).

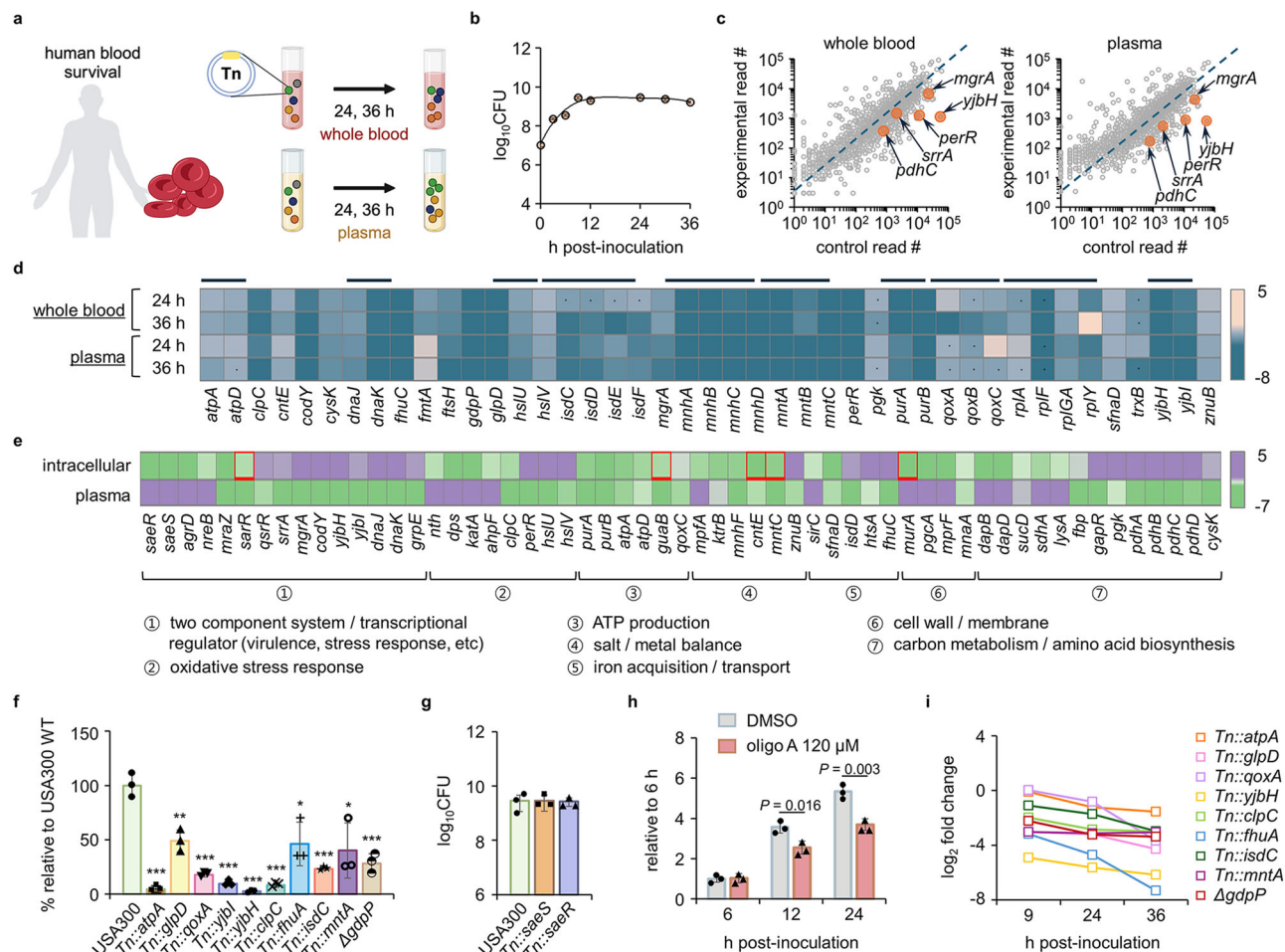


**Fig. 4 | Tn-seq reveals a set of genes specifically essential for blood survival of *S. aureus*.** **a** The USA300 Tn library was cultured in human whole blood and plasma for 24 and 36 h, after which the bacteria were collected and prepared for Tn-seq. Image created in BioRender (Lee, W. (2025) <https://BioRender.com/gwn8ee3>).

**b** The growth of USA300 was examined for 36 h. **c** Gene read counts from a 24 h post-inoculation sample were compared to those of the Tn library grown in TSB. Representative genes from the list of substantially depleted genes are presented on the plot. **d** Representative genes depleted in whole blood and plasma are expressed as a heat map (dots: genes that meet the  $\log_2$  fold change criterion but not the  $P$  value criterion; black lines: gene groups). **e** Representative genes required for intracellular (2 h) and plasma (36 h) survival are compared (red squares: genes for which the 4 or 8 h post-infection read counts were used since they were either

defined as late essential or were not depleted at 2 h but rather at other time points). The mutants of selected genes were validated for their **(f)** essentiality and **(g)** non-essentiality for survival in whole blood. The mutants were cultured in whole blood for 24 h, and CFU were counted to measure the survival. \*  $P < 0.05$ ; \*\*  $P < 0.01$ ; \*\*\*  $P < 0.001$  compared to the USA300 strain. The exact  $P$  values are available in the **Source Data** file. **h** USA300 pre-exposed to 120  $\mu$ M of oligomycin A (oligo A) was placed into whole blood in the presence of oligomycin A to investigate the essentiality of ATP production for blood survival. Data in **b** and **f–h** are presented as the mean  $\pm$  SD ( $n = 3$  biological replicates), and the  $P$  values are calculated by a two-sided, unpaired Student's  $t$ -test. **i** The  $\log_2$  fold change of the mutants of genes essential for blood survival was expressed in a time course up to 36 h post-blood inoculation. Source data for **b**, **c** and **f–i** are available in the **Source Data** file.

## *S. aureus* in human blood remodels its metabolism to allow simultaneous utilization of lactate and glucose

Next, we sought to identify key metabolic pathways involved in bacterial survival and growth in human blood. Since human blood contains distinct nutrients, particularly the available carbon sources, and since carbon source utilization is pivotal for bacterial survival, we have re-evaluated our Tn-seq data from this perspective. Interestingly, in the blood samples we found a substantial enrichment of reads due to the Tn insertions in *ccpA*, which is involved in catabolic repression in *S. aureus* (Fig. 5a). We confirmed this enrichment by using a *ccpA* deletion mutant, which exhibited enhanced growth in human blood (Fig. 5b, c) with the growth profile in TSB shown in Supplementary Fig. 11c, d. CcpA regulates a selective utilization of carbon sources when multiple carbon sources are available<sup>34,35</sup>. This result led us to investigate the nutrient composition in human blood. We focused on carbon sources that directly enter glycolysis and the TCA cycle, which include amino acids, glucose, and lactate. As previously reported, we found that

human blood contains high concentrations of glucose (0.8 mM), lactate (1.3 mM), and amino acids (Supplementary Fig. 12)<sup>36</sup>. First, we examined the consumption of carbon sources by *S. aureus* in blood. As shown in Fig. 5d, *S. aureus* simultaneously consumed lactate and glucose. Typically, bacteria prefer glucose over lactate or acetate when both carbon sources are available, and this is regulated by catabolic repression<sup>37–39</sup>. When we monitored carbon source consumption in TSB media containing both 10 mM glucose and 10 mM lactate, we observed a typical pattern in which *S. aureus* initially consumed glucose until it was depleted and then began to utilize lactate (Fig. 5e). The simultaneous utilization of carbon sources has also been observed in *Mycobacterium tuberculosis*<sup>40,41</sup>. However, unlike *M. tuberculosis*, *S. aureus* exhibited the ability to adapt its mode of catabolic repression and shifted to a simultaneous mode only in the host environment, which conferred a fitness advantage.

Additionally, we monitored the concentrations of amino acids during the 24-h blood culture and observed that *S. aureus* actively



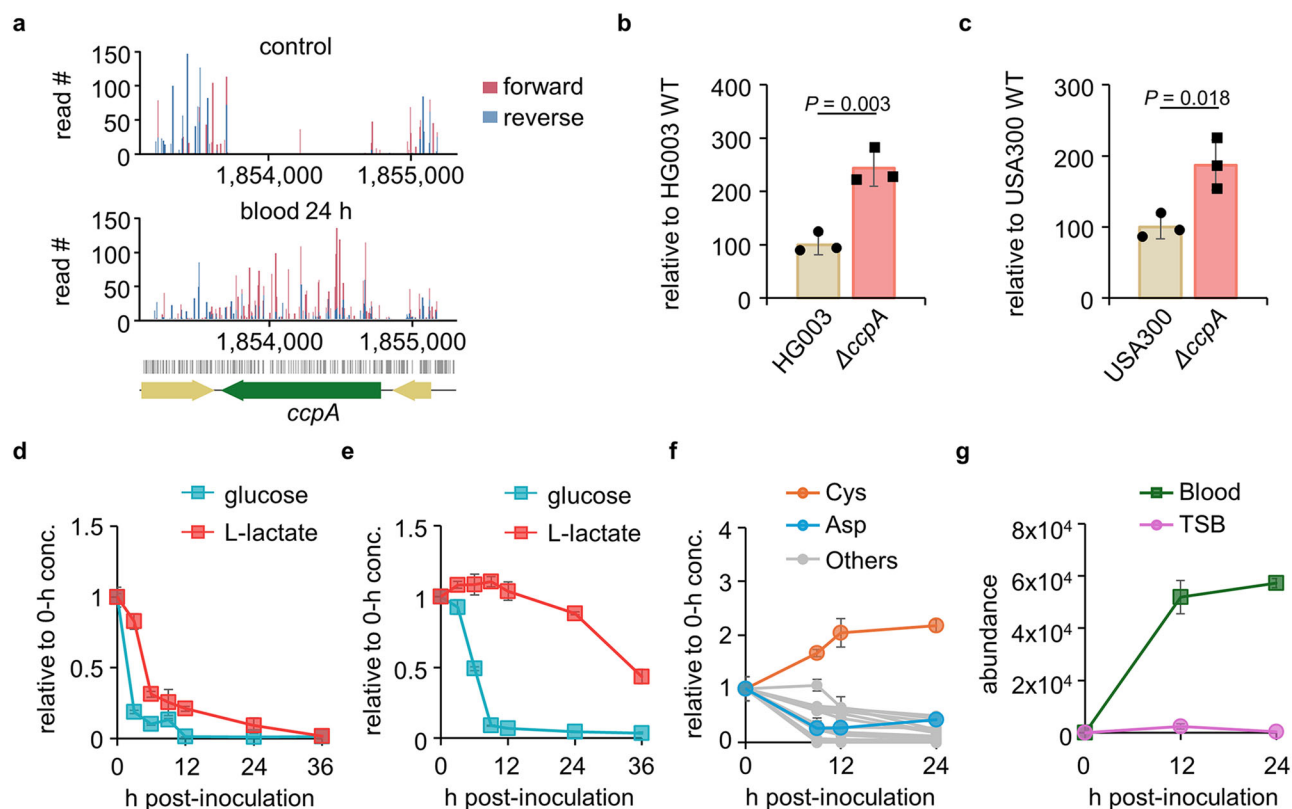


**Fig. 5 | *S. aureus* simultaneously utilizes lactate and glucose in blood.** **a** The read counts for all TA sites within the *ccpA* gene detected by sequencing in both forward (red) and reverse (blue) directions were plotted using R. For identification of the role of the *ccpA* gene for bacterial growth in blood, *ΔccpA* strains generated in **(b)** HG003 and **(c)** USA300 strains were cultured in blood for 24 h and were counted for CFU. WT; wild-type. For the measurement of lactate and glucose consumption of USA300 in blood and TSB, bacteria were cultured in **(d)** blood or **(e)** TSB for up to 36 h. At designated time points, blood and TSB samples were centrifuged for the collection of plasma and supernatant, respectively, which were prepared for mass spectrometric analysis. **f** USA300 was cultured in human whole blood for up to 36 h for the measurement of amino acid consumption. At designated time points, blood was centrifuged for plasma collection and prepared for mass spectrometric

analysis (others include Ala, Arg, Asn, Glu, Gln, His, Leu, Lys, Met, Phe, Pro, Thr, Trp, Tyr, and Val). **g** For the measurement of bacterial bacillithiol, USA300 was inoculated into human whole blood or TSB for 9, 12, or 24 h. At designated time points, samples were centrifuged for the collection of bacterial cells, after which the bacterial cells were quenched, lysed by bead beating, and prepared for mass spectrometric analysis. Bacillithiol levels at each time point were normalized to  $\log_{10}$  bacterial CFU. Glucose, lactate, amino acid concentrations, and bacillithiol levels in **d–g** were measured using LC/MS-TOF, and the abundance of extracted metabolite ion intensities was acquired using Profinder 6<sup>50</sup>. All data in **d–g** are presented as the mean  $\pm$  SD ( $n = 3$  biological replicates). Source data is available in the **Source Data** file.

consumed all amino acids except cystine (Fig. 5f). Interestingly, we found that *S. aureus* produced cystine over two-fold compared to the control. In line with this data, we identified substantial depletion of *cysK*, the final enzyme in cysteine biosynthesis, suggesting the essentiality of this gene for survival in the blood environment (Fig. 4d)<sup>42</sup>. The *cysK* is the only gene we found related to amino acid biosynthesis, further validating the results of cystine increase in blood. Interestingly, in blood, we found that genes such as *perR*, *trxB*, and *hslUV* were substantially depleted in the blood environment, indicating that *S. aureus* experiences oxidative stress in blood. Bacterial thiols act as protective agents against oxidative stress, and in *S. aureus* these include bacillithiol (N-cysteinyl- $\alpha$ -D-glucosaminyl-L-malate), a hexamine conjugated to L-cysteine<sup>43,44</sup>. Indeed, aligned with the cysteine accumulation results, we observed that bacillithiol levels increased sustainably over time in the USA300 strain cultured in blood. However, we found only a minimal increase in the intracellular bacillithiol levels in USA300 during the stationary phase when cultured in TSB (Fig. 5g). Therefore, the depletion of genes related to oxidative stress is consistent with the requirement of *cysK* and the accumulation of cysteine and bacillithiol in the blood environment. To survive in blood, *S. aureus* depends on genes related to response to oxidative stress, including those associated with bacterial thiol synthesis. Furthermore, our results indicate that *S. aureus* adjusts its metabolism to better adapt to

the extracellular host environment, allowing for more efficient utilization of available carbon sources and response to oxidative stress.

### The genes required for invasion into the liver or lungs show substantial overlap with the genes important for extracellular survival of *S. aureus*

Next, we attempted to identify how *S. aureus* adapts to different host organs. For this, we decided to use a mouse USA300 infection sepsis model. First, we tested different CFU administered through the tail vein and chose the dose resulting in an 83% survival rate at 48 h post-infection. For Tn-seq, based on the dose, we infected a total of  $2 \times 10^8$  CFU of the USA300 Tn library, and after 24 h, we separately recovered the surviving Tn mutants from six organs for sequencing (Fig. 6a). Among these six organs, the CFU from the kidneys were the highest, while those of the heart, brain, and spleen were lower, as expected. However, interestingly, in our Tn-seq analysis, we found a very low diversity of Tn mutants in the kidneys. This suggests that the kidneys are relatively hard to infect, but mutants able to do so may encounter a less hostile growth environment than in other organs. In contrast, we recovered a low count of CFU in the spleen, but the mutants were relatively more heterogeneous than in the kidneys, suggesting that there is a lower bottleneck to entry but an unfavorable environment inside the spleen for *S. aureus* replication. For a numerical

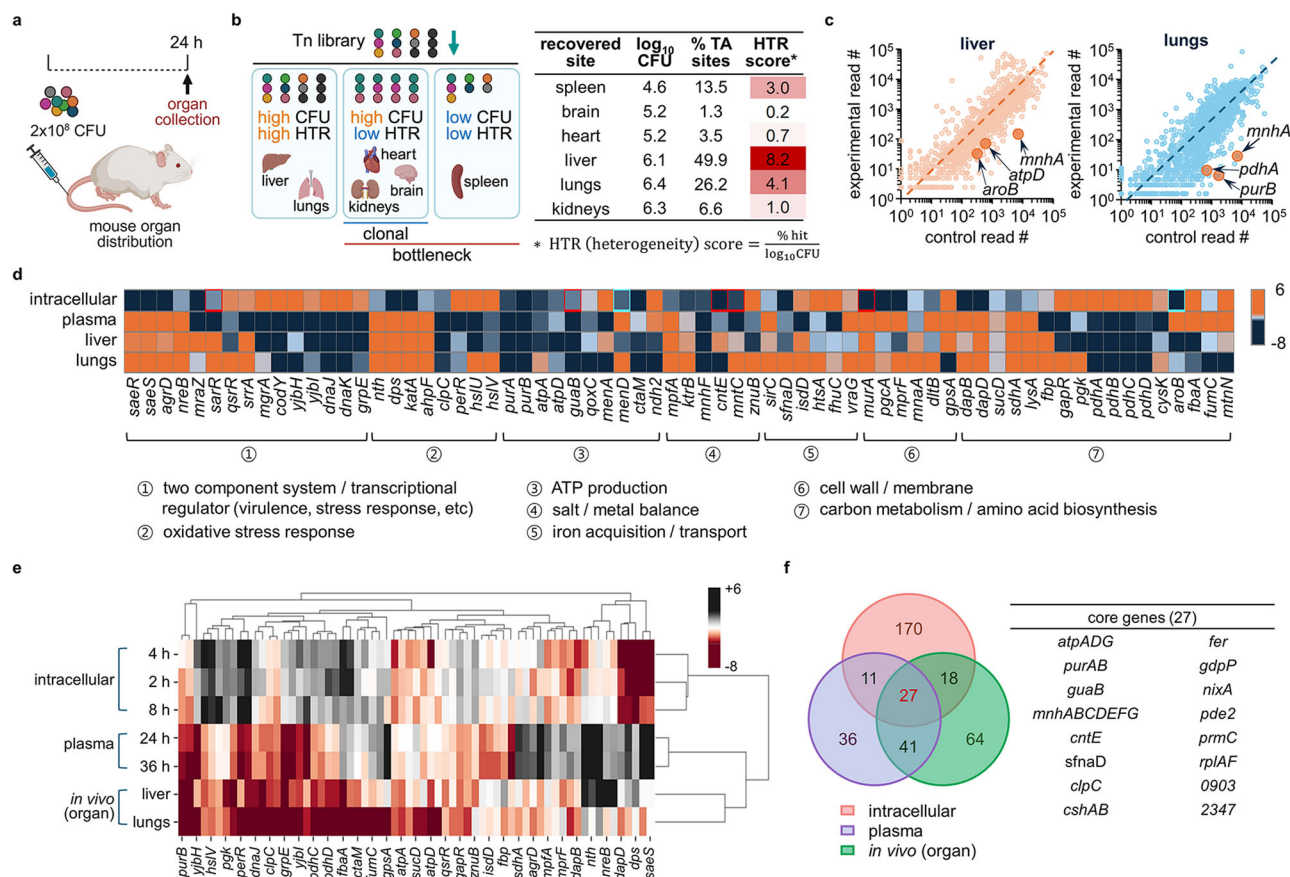


**Fig. 6 | Mouse sepsis model reveals sets of genes essential for the establishment of *S. aureus* invasion into organs.** **a** Mice (BALB/c, 8-week-old, male) were infected with  $2 \times 10^8$  CFU of the USA300 Tn library via tail vein injection. Mice were euthanized at 24 h post-infection upon which organs were collected and prepared for Tn-seq. Image created in BioRender (Lee, W. (2025) <https://BioRender.com/c70829c>). **b**  $\log_{10}$  of bacterial CFU, % TA sites (TA sites detected in experimental samples out of all the TA sites in the genome), and HTR scores ( $\frac{\% \text{ TA sites}}{\log_{10} \text{ CFU}}$ ) are presented in a table. The organs were classified into three groups (high CFU ( $\log_{10} \text{ CFU} > 5$ ) – high HTR ( $\text{HTR} > 4$ ); high CFU – low HTR ( $\text{HTR} < 4$ ); low CFU ( $\log_{10} \text{ CFU} < 5$ ) – low HTR). Image created in BioRender (Lee, W. (2025) <https://BioRender.com/ng111mx>). **c** Gene read counts from lungs and liver were plotted against the read counts of the respective genes of a control Tn library. Representative genes are marked on the plot. Source data is available in the **Source Data** file. **d** Genes essential for intracellular survival

(2 h), plasma survival (36 h), and survival in organs (both liver and lungs) are compared in a heat map (red squares: genes for which the 4 or 8 h post-infection read counts were used because they were either defined as late essential or were not depleted at 2 h but rather at other time points; blue squares: genes for which the 0 h read counts were used because they were defined as early essential). **e** Gene clustering analysis was performed using the Seaborn, clustermap Python package (v.0.12.2) using all genes from **d**, but *aroB*, *menA*, and *menD* were excluded since they were early essential genes that do not appear at 2, 4, or 8 h post-infection. **f** The numbers of genes that are specifically and commonly essential for intracellular, blood, and organ survival are presented in a Venn diagram, and the 27 core genes that are essential for infection in all three host environments (intracellular, blood, and intra-organ) are listed in a table.

representation of these data, we have generated a heterogeneity (HTR) score by normalizing % TA sites (TA sites detected in experimental samples out of all the TA sites in the genome) by the total recovered CFU from each organ (Fig. 6b). Higher HTR means higher diversity of recovered mutants. Using the counts of CFU and HTR scores, we categorized the six organs into three groups: (I) high CFU and high HTR (liver and lungs), (II) high CFU and low HTR (heart, kidneys, brain), and (III) low CFU and low HTR (spleen). Group I includes organs that show high recovery of CFU ( $\log_{10} \text{ CFU} > 5$ ) and diversity of mutants (HTR score  $> 4$ ), implying little physical barrier for bacterial invasion and survival. Group II includes organs with high CFU but low HTR (score  $< 4$ ), suggesting that a bottleneck limited mutant entry. Permissive growth conditions after the bottleneck resulted in a clonal mutant population. Group III includes the spleen, which shows low CFU ( $\log_{10} \text{ CFU} < 5$ ) with low HTR, implying that this organ provides an unfavorable environment for both entry and growth of bacteria. Since bottlenecks limit genetic diversity in the mutant pools for organs in groups II and III, we focused on organs in group I, the liver and lungs, which showed a high CFU with HTR score  $> 4$ , for further gene analysis. In addition, because *S. aureus* is common in lung infections, data

generated from the lungs may be of clinical relevance<sup>45</sup>. Tn data for each organ identified 119 depleted genes for liver and 81 depleted genes for lungs (liver –  $\log_2$  fold change  $\leq -2$  with  $P$  value  $\leq 0.01$ ; lungs –  $\log_2$  fold change  $\leq -4$  with  $P$  value  $\leq 0.01$ ) (Fig. 6c and Supplementary Fig. 13).

As shown in Fig. 6d, in both organs we identified genes encoding TCSs and associated regulators, including *mgaA* and *yjb* locus. We also found genes for ATP production (*atp* locus, *qoxC*, and *ndh2*) and genes related to the oxidative stress response (Fig. 6d, groups 2 and 3). Notably, the oxidative stress response genes found to be important in the liver and lungs were different from those involved in intracellular survival. Similarly, TCS SaeRS and cell wall biosynthesis and metabolism-associated genes (*mpfA*, *muraA*, *lysA*, and *dapB*) were depleted only in an intracellular environment but not in blood and intra-organ environments. Most genes depleted in the liver and lungs were shared, but several, such as *copZ* and *gpsA*, were depleted only in the lungs (Supplementary Fig. 13), and the essentiality of the functional groups was further validated by the operon analysis (Supplementary Fig. 14). The essentiality of genes was confirmed with the *atpD* mutant being less infective in both liver and lungs (Supplementary Fig. 15a),



while *copZ* and *pyrE* genes were only essential for lung or liver infection, respectively (Supplementary Fig. 15b, c). In addition, the mice infected with the *atpD* mutant showed improved survival compared to the mice infected with wild-type USA300 (Supplementary Fig. 15d), implying that an *atp* locus could serve as an effective therapeutic target for the treatment of bacterial infection. All these results were obtained with no apparent growth defects in the mutants (Supplementary Fig. 15e). When we compared the genes found to be important in the lungs or liver with those involved in the intracellular and extracellular milieus, we found that the set of genes identified as essential for survival in these organs resembled those required for extracellular survival (Fig. 6d) and as analyzed by the clustering analysis (Fig. 6e). Genomic profiling using the in vivo sepsis model is a conglomeration of results from the blood, tissue, and intracellular bacteria. Therefore, the results from bacteria recovered from organs might be skewed by the bacteria remaining in the extracellular and tissue environments.

All three systems, intracellular, extracellular, and intra-organ, required sets of genes involved in ATP production and maintenance of nutrient and ion balance, resulting in 27 core genes (Fig. 6f). These results indicate that ATP production and nutrient/ion balance are essential for growth in any given environment, despite other differences in each host niche.

## Discussion

Our study demonstrates that *S. aureus* can adapt differentially within various host niches to exploit nutrients and respond to hostile conditions. It does so by employing both metabolic changes and regulators that serve as hubs for signal relay for many virulence-related genes, and this shaping of the metabolic and physiological makeup of *S. aureus* is crucial for survival and response to host environmental cues. These differential environmental cues vary depending on whether *S. aureus* is in an intracellular, extracellular, or intra-organ environment.

Here, we used three infection models—a cell culture model, blood, and a mouse model focusing on specific organs—to identify genes necessary for survival within the host. Despite residing on the skin, which constitutes an extracellular environment, *S. aureus* is fully equipped to thrive intracellularly and within organs<sup>9,16–18,46</sup>. In our Tn-seq analysis using the mouse sepsis model, our approach involved assigning a heterogeneity score to each organ, revealing distinct characteristics for each. For example, *S. aureus* showed the largest bacterial count but a highly clonal population in the kidneys, suggesting that only certain mutants can infiltrate into the kidneys or, alternatively, that most mutants are filtered out of the kidneys, but a small number of mutants attach to the organ and multiply. On the contrary, in the lungs and liver, where bacteria also grew to a high count, *S. aureus* showed high heterogeneity, suggesting that these organs are accessible to most mutants. Notably, *S. aureus* primarily enters the lungs via the respiratory route rather than the bloodstream, but regardless of the mode of entry, the lungs are highly accessible to *S. aureus*<sup>47</sup>. Therefore, we conclude that these organs are extremely vulnerable to bacterial infection and provide a favorable niche for bacterial survival. In the spleen, *S. aureus* shows both low bacterial count and low heterogeneity, which might be expected from an organ rich in macrophages. Unexpectedly, a high bacterial count was found in the brain, an organ that is protected by the blood-brain barrier. This finding suggests that there is a route for *S. aureus* entry into the brain parenchyma, but as can be seen from the low heterogeneity, only certain mutants can do so. These findings demonstrate the potentially different levels of barriers and protection presented by each organ during systemic *S. aureus* infections, highlighting distinct environmental characteristics that allow for *S. aureus*

replication. Our results may suggest which organ is most vulnerable during *S. aureus* sepsis.

By studying the bacterial interaction with human blood and comparing the gene sets essential for survival in whole blood and plasma, we demonstrate that bacteria do not invade the RBC. Since the human blood used in this study was commercially sourced and treated with heparin, with immune cells mostly deactivated, the Tn-seq results for blood can apply to the general extracellular body fluid encountered by the bacteria once inside the host body. We have particularly shown that the essentiality of genes responsible for response to oxidative stress along with the increased production of bacillithiol in *S. aureus* upon incubation in blood implies the importance of the stress response pathways for survival in the blood environment. In addition, our organ data resembled the extracellular results in blood, suggesting that once inside the organs, a large population of *S. aureus* resides in an extracellular body fluid rather than inside the cells.

Regulators such as SaeRS, AgrA, SarA, SrrA and MgrA are known to be required during *S. aureus* infection<sup>10–13</sup>. However, our findings suggest that they are differentially required in specific host niches and not consistently across all environments, which should be considered in mapping their signal relay. On the other hand, we found that in all three infection systems, 27 core genes, such as ATP synthase and the *mrh* antiporters, required for nutrient processing, are crucial for survival within the host. Our study implies that energy metabolism plays an essential role in bacterial survival, regardless of the host niche. Valentino et al. also utilized Tn-seq for the identification of genes essential for survival in skin abscess<sup>48</sup>. These authors showed that several genes involved in the pyrimidine and purine biosynthesis pathways are critical for survival in skin abscesses; and some of these genes, such as *purB* and *guaB*, were also identified as essential in bacterial survival in all biological systems (intracellular, extracellular, and intra-organ) used in the current study. This similarity indicates that energy metabolism is a possible therapeutic target for combating *S. aureus* infection. It has also been shown that the *cydABCD* locus and polysaccharide pathway of *E. faecalis* are crucial for adaptation and survival in the bloodstream<sup>49</sup>. Therefore, a broader understanding of metabolic reprogramming during infection can be crucial for suppressing the growth of bacterial pathogens in the host environment. A comprehensive and comparative understanding of the underlying mechanisms responsible for the establishment of bacterial infection in different host niches will greatly contribute to the development of efficient treatment strategies.

## Methods

### Ethics statement and animal information

Mouse experiments were approved by and performed in strict accordance with the institutional guidelines of the Institutional Animal Care and Use Committee of Sungkyunkwan University School of Medicine (approval number: SKKUIACUC2021-11-35-1). All animal experiments were performed in a facility approved for BSL-2 experiments involving a bacterial Tn library. Male, 7-week-old BALB/c mice were purchased from Orient Bio (Seongnam, South Korea) and acclimated to an animal facility isolated for infection studies at Sungkyunkwan University School of Medicine. All mice were maintained under pathogen-free conditions on a 12:12 h light:dark cycle, with free access to facility chow and water. The temperature and humidity of the facility were maintained at 22 °C and 50%, respectively. The experiments performed with human blood were all approved by the Sungkyunkwan University Institutional Review Board (IRB: SKKU 2023-01-023).

### Cell lines and culture conditions

The lung epithelial cell line A549 (Korean Cell Line Bank, Seoul, South Korea; #10185) was grown in Roswell Park Memorial Institute 1640 (RPMI 1640) medium (Welgene, Gyeongsan, South Korea) supplemented with 10% fetal bovine serum (FBS; Welgene). The murine

macrophage cell line Raw264.7 (Korean Cell Line Bank; #40071) and human keratinocyte cell line HaCaT (Cellular Engineering Technologies, Coralville, IA; #CR1017-500) were maintained in Dulbecco's Modified Eagle's Medium (DMEM; Welgene) supplemented with 10% FBS. All cell lines were grown in a humidified 37 °C, 5% CO<sub>2</sub> incubator and sub-cultured by trypsinization.

### Bacterial strains and culture conditions

Methicillin-resistant *S. aureus* (MRSA) strains USA300, MW2, and MRSA252, and methicillin-sensitive *S. aureus* (MSSA) strains HG003, MSSA476, and Newman strains were grown at 30 °C in liquid tryptic soy broth (TSB; Beckton Dickinson, Franklin Lakes, NJ) with shaking or on agarized TSB plates (TSA). Mutant strains obtained from the Nebraska transposon mutant library (NTML) were grown in liquid TSB or TSA with the addition of 10 µg/mL erythromycin (Erm; Sigma-Aldrich, Burlington, MA). The mutant strains used in the study are summarized in Supplementary Table 1, and all mutants were confirmed for the Tn insertion at the target gene using primers (Macrogen, Seoul, South Korea) as detailed in Supplementary Table 2. On the day of an experiment, an overnight bacterial culture was re-inoculated at OD<sub>600</sub> = 0.01 and grown until OD<sub>600</sub> = 0.4–0.6. The transposon mutant library (Tn library) was created in USA300 by phage-based transposition as previously described<sup>24</sup>. Library aliquots were stored at –80 °C and on the day of the experiment were grown from OD<sub>600</sub> = 0.2 to OD<sub>600</sub> = 0.4 for no more than 3 h.

### Generation of mutants of *S. aureus*

For a generation of *ΔmnhF* and *ΔccpA*, DNA fragments corresponding to 1 kb upstream and downstream of *mnhF* and *ccpA* were amplified with the primer pairs *mnhF1/mnhF3* and *mnhF2/mnhF4* for *mnhF* and *ccpA1/ccpA3* and *ccpA2/ccpA4* for *ccpA* (Supplementary Table 2). The kanamycin (Km) resistant gene was amplified with the primer pair KmF/KmR. Following purification, the Km-resistant fragment was combined with the *mnhF* and *ccpA* fragments using KOD Xtreme Hot Start DNA polymerase (Novagen, Madison, WI) with the primer pairs *mnhF5/KmR* and *mnhF5/mnhF6* for *mnhF* and *ccpA5/KmR* and *ccpA5/ccpA6* for *ccpA* (Supplementary Table 2). The combined PCR product was digested with BamHI/HindIII and BamHI/Sal for *mnhF* and *ccpA*, respectively, and the resulting products were cloned into pKFC (pKFC-*delmnhF* and pKFC-*delccpA*) and transformed into electrocompetent *S. aureus* RN4220, resulting in the generation of RN4220-*ΔmnhF* and RN4220-*ΔccpA*. Homologous recombination was performed to integrate the plasmid into the bacterial chromosome, and the deletion of the target gene was confirmed by sequencing. Confirmed deletions were transduced using φ11 into HG003 and USA300 to generate HG003-*ΔmnhF*, HG003-*ΔccpA*, USA300-*ΔccpA*<sup>50</sup>. All bacterial strains, primer sequences, and plasmids are summarized in Supplementary Tables 1 and 2.

### Determination and validation of genes essential for intracellular infection

**Intracellular infection assay.** To determine the extent of intracellular infection and survival of *S. aureus*, host cells were seeded in the T25 cell culture flasks at  $3.5 \times 10^6$  cells/flask or the 24-well culture plates at  $2.5 \times 10^5$  cells/well and placed in a humidified 37 °C, 5% CO<sub>2</sub> incubator for 48 h. At 1 h before bacterial infection, the culture medium was replaced with fresh medium. The bacterial strains were grown to a log phase and added to the host cell culture medium at a multiplicity of infection (MOI) of 10 as per the result for screening for MOI that resulted in full recovery of input bacteria. After 1.5 h of infection, bacteria-containing culture medium was removed, and host cells were washed five times with sterilized PBS. Afterwards, medium containing 200 µg/mL gentamicin was added for 1 h to remove extracellular bacteria, after which the host cells were again washed 5 times with sterilized PBS. The host cells were immediately (time point designated as

0 h post-infection throughout the manuscript) lysed with 0.1% Triton X-100, and the collected bacteria were spread on TSA plates and grown at 30 °C for counting of bacterial colony-forming units (CFU). For examination of post-entry events, fresh culture medium was added to the flask after the removal of gentamicin-containing medium and washing with PBS, and host cells were lysed at 2, 4, and 8 h post-addition of fresh medium (time points designated as 2, 4, and 8 h post-infection throughout the manuscript). Bacteria were spread on TSA plates and grown at 30 °C for counting of bacterial CFU. The protocol was adapted and modified from previous publications<sup>51–53</sup>.

**Tn library infection experiment.** For the determination of genes essential for intracellular entry and post-entry survival, an infection assay of the USA300 Tn library into host A549 cells was performed. Host A549 cells were seeded in T25 cell culture flasks at  $3.5 \times 10^6$  cells/flask, and the Tn library was grown to OD<sub>600</sub> = 0.4 as described above. The infection procedure was performed as described above. The host cells were lysed at 0, 2, 4, and 8 h post-entry and spread on TSA+Erm (10 µg/mL) plates and grown at 30 °C. The colonies were then scraped and pooled for preparation for the transposon sequencing (Tn-seq).

**Validation assay with mutants.** To validate the results obtained from the Tn library infection assay, individual mutants were tested for the extent of their intracellular entry and post-entry survival<sup>54</sup>. All mutants are listed in Supplementary Table 1 and were confirmed for the Tn insertion at the target gene using primers as detailed in Supplementary Table 2. For validation, host A549 cells were seeded in 24-well culture plates at  $2.5 \times 10^5$  cells/well, and the rest of the procedure was the same as outlined above for the intracellular infection assay. Upon lysis of host cells at 0, 2, 4, and 8 h post-entry, mutants were spread on TSA plates containing appropriate antibiotics and counted for the number of colonies at each time point.

**Confirmation of the effects of an ATPase inhibitor on bacterial intracellular entry and post-entry survival.** For the determination of the effects of ATPase inhibition, USA300 was cultured in media containing 120 µM of oligomycin A (Sigma-Aldrich) for 4 h<sup>32</sup>. Then, bacteria pre-treated with oligomycin A were utilized for the intracellular infection assay. A549 cells were exposed to bacteria pre-treated with oligomycin A, also in the presence of 120 µM oligomycin A during infection and throughout the experiment until A549 cell lysis at various time points. Upon lysis of host cells at 0, 2, 4, and 8 h post-entry, the bacteria were spread on TSA plates and counted for the number of colonies at each time point.

### Determination and validation of genes essential for survival in human blood/plasma

**Human blood/plasma survival assay.** To determine the bacterial growth and survival in human blood, human blood anticoagulated with heparin was purchased from Innovative Research (Novi, MI) through an FDA-approved collection center in the USA. To separate plasma, whole blood was centrifuged at  $845 \times g$  at 4 °C for 15 min, after which the supernatant was obtained. Whole blood and plasma were placed into 14-mL round-bottom tubes in 2-mL aliquots. The bacterial strains were grown to a log phase and added to the human whole blood or plasma at a final OD<sub>600</sub> = 0.02. Whole blood and plasma were incubated at 37 °C, with shaking at 150 rpm for 24 or 36 h. The samples were then placed in red blood cell (RBC) lysis buffer (10×; 1.5 M NH<sub>4</sub>Cl, 100 mM NaHCO<sub>3</sub>, 1 mM EDTA, pH 7.4) and spread on TSA plates for CFU counting.

**Tn library infection into human blood and plasma.** For the determination of genes essential for the survival of USA300 in human blood, whole blood and plasma were prepared as outlined above and placed into 14-mL round-bottom tubes in 4-mL aliquots. The Tn library was

grown to  $OD_{600} = 0.4$  and added to the human whole blood and plasma at a final  $OD_{600} = 0.02$ . Whole blood and plasma were incubated at  $37^{\circ}\text{C}$ , with shaking at 150 rpm for 24 and 36 h. After 24 and 36 h of growth, samples were placed on ice. RBC lysis buffer was added at a volume of 4 mL and incubated for 10 min to lyse RBC in whole blood samples. Both whole blood (now with lysed RBC) and plasma samples were centrifuged at  $9391 \times g$  at  $4^{\circ}\text{C}$  for 5 min and washed 3 times with sterilized PBS. The resulting pellet was used for preparation for Tn-seq.

**Validation assay with mutants.** To validate the genes found essential in the blood and plasma survival assay, individual mutants were tested for the extent of their blood survival. All mutant strains are listed in Supplementary Table 1 and were confirmed for the Tn insertion at the target gene using primers as detailed in Supplementary Table 2. For the validation assay, whole blood was placed into 14-mL round-bottom tubes in 2-mL aliquots into which the mutants were inoculated at an initial  $OD_{600} = 0.02$ . The tubes were placed at  $37^{\circ}\text{C}$ , with shaking at 150 rpm for 24 h after which the bacteria were spread on TSA plates containing appropriate antibiotics and counted for the number of colonies.

**Validation of effects of ATPase inhibition on bacterial blood survival.** For the determination of the effects of ATPase inhibition, USA300 was cultured in media containing  $120 \mu\text{M}$  of oligomycin A (Sigma-Aldrich) for 4 h. Then, the bacteria pre-treated with oligomycin A were added to human blood at an  $OD_{600} = 0.02$ , also in the presence of  $120 \mu\text{M}$  oligomycin A. After 6, 12, and 24 h of growth, the bacteria were spread on TSA plates and counted for the number of colonies appearing at each time point.

### Determination and validation of genes essential for an intra-organ survival

**Tn library infection into the mouse sepsis model.** For the identification of genes essential for bacterial survival in the organs, a mouse sepsis model was used<sup>55</sup>. Animals were injected with a USA300 Tn library at  $2 \times 10^8$  CFU per mouse by intravenous injection with an injection volume of  $100 \mu\text{L}$ . For this, the Tn library (grown to  $OD_{600} = 0.4$  as described above) was resuspended in sterilized phosphate-buffered saline (PBS) used as an injection medium. At 24 h post-bacterial injection, animals were euthanized by isoflurane overdose, followed by exsanguination and organ collection for analysis. At collection, the spleen, brain, heart, liver, lungs, and kidneys were homogenized in PBS containing 0.1% Triton X-100 (Sigma-Aldrich), after which the homogenate was spread on TSA+Erm ( $10 \mu\text{g/mL}$ ) plates and grown at  $30^{\circ}\text{C}$  for bacterial colony collection for Tn-seq.

**Validation assay with NMTL mutants.** To validate the results obtained from the Tn-seq of the organs, individual mutants obtained from the NMTL were tested for the extent of their survival in the lungs and liver. All mutants are listed in Supplementary Table 1 and were confirmed for the Tn insertion at the target gene using primers as detailed in Supplementary Table 2. Briefly, mice were injected with individual NMTL mutants or wild-type USA300 at  $2 \times 10^8$  CFU/mouse by intravenous injection with an injection volume of  $100 \mu\text{L}$ . At 24 h post-injection, mice were euthanized, and organs (lungs and liver) were collected and homogenized. The samples were spread on TSA+Erm ( $10 \mu\text{g/mL}$ ) plates and grown at  $30^{\circ}\text{C}$  after which the numbers of CFU on the plates were counted.

### Tn-seq and data analysis

A Tn library grown on TSA+Erm ( $10 \mu\text{g/mL}$ ) plates obtained from the intracellular infection study, blood/plasma survival study, and the mouse sepsis study was scraped, and genomic DNA was harvested and prepared for deep sequencing as previously outlined<sup>24</sup>. Illumina high-

throughput sequencing was performed on a Hi-Seq2000 or Hi-Seq2500 for 100 cycles with 40%  $\Phi\text{X}174$  spiked into the sequencing reaction (Macrogen). The sequencing data were trimmed, filtered, and processed using the Galaxy software suite. The chromosome nucleotide FASTA file for USA300-TCH1516 (NC\_010079.1) was downloaded from the NCBI Genome database, and the obtained sequencing data were mapped to the genome using Bowtie software. Python scripts were used to compare the number of reads in the control and experimental conditions using the Mann-Whitney U test, correcting for multiple hypothesis testing with the Benjamini-Hochberg procedure. An EL-ARTIST essential gene analysis was done in MATLAB. The essentiality threshold was set to  $P$  value  $\leq 0.05$  after correcting for the false discovery rate. The operon analysis of the Tn-seq data was performed using Rockhopper (v.2.0.3)<sup>56</sup>.

### Transmission electron microscopy

For transmission electron microscopy (TEM) imaging, A549 cells were seeded in  $\Phi 15$  mm glass-bottom cell culture dishes (Nest Scientific, Rahway, NJ) at a density of  $7 \times 10^5$  cells/plate and incubated in a humidified  $37^{\circ}\text{C}$ , 5%  $\text{CO}_2$  incubator for 48 h. At 1 h before infection, the cell culture medium was changed to fresh medium, after which USA300 (grown to  $OD_{600} = 0.4$ – $0.6$ ) was added to the culture medium at an  $\text{MOI} = 10$  for infection lasting 1.5 h, followed by washing ( $5\times$  with sterilized PBS) and 1 h treatment with gentamicin  $200 \mu\text{g/mL}$ . Cells were then again washed  $5\times$  with PBS, and fresh RPMI 1640 medium was added, after which cells were placed in a humidified  $37^{\circ}\text{C}$ , 5%  $\text{CO}_2$  incubator for 4 h. At 4 h post-incubation, the sample was fixed in 2.5% glutaraldehyde solution for 1 h at room temperature. The blood samples were generated by culturing USA300 in human whole blood from an initial  $OD_{600} = 0.02$  for 4 and 12 h at  $37^{\circ}\text{C}$ , with shaking at 150 rpm. At designated time points, samples were centrifuged at  $9391 \times g$  at  $4^{\circ}\text{C}$  for 5 min and washed with sterilized PBS three times. Then, the samples were fixed in 2.5% glutaraldehyde solution for 1 h at room temperature. Both cell and blood samples were then dehydrated with an ethanol series and infiltrated with Spurr's resin series, after which the samples were polymerized for 8 h at  $60^{\circ}\text{C}$ . The sample-embedded blocks were cut with a diamond knife on an ultramicrotome (Leica Microsystems, Wetzlar, Germany), and the resulting sections were directly mounted on 150 mesh copper grids. The sections were stained for 20 min with 2% uranyl acetate in 50% methanol, followed by staining with Reynold's lead citrate for 10 min. The grids were imaged in a bio-imaging core facility of Korea Institute of Science and Technology (KIST) using Tecnai F20 G2 (FEI, Hillsboro, OR) equipped with a RIO 16 camera under the magnification of  $17,000\times$  to  $65,000\times$ .

### Fluorescence microscopy

**Preparation of FtsZ-GFP expressing USA300 strain.** The pLow-ftsZ-GFP plasmid was inserted into the RN4220 strain by electroporation using a GenePulser cuvette (BioRad, Hercules, CA) at a voltage of 2900 V, 25  $\mu\text{F}$  capacitance, 100  $\Omega$  resistance, and 2 mm length<sup>57</sup>. After electroporation, FtsZ-GFP-expressing RN4220 (RN4220-FtsZ-GFP) colonies were selected on TSA+Erm ( $10 \mu\text{g/mL}$ ) at  $30^{\circ}\text{C}$ . The pLow-ftsZ-GFP was then transduced into USA300 using staphylococcal phage  $\phi 11$ , generating the FtsZ-GFP-expressing USA300 strain (USA300-FtsZ-GFP). Details of all strains and plasmids can be found in Supplementary Tables 1 and 2.

**Fluorescence microscopy.** The obtained USA300-FtsZ-GFP was used to visually inspect and analyze bacterial infection into and survival in host cells. For imaging, A549 cells were seeded in  $\Phi 15$  mm glass-bottom cell culture dishes (Nest Scientific) at  $7 \times 10^5$  cells/plate and incubated in a humidified  $37^{\circ}\text{C}$ , 5%  $\text{CO}_2$  incubator for 48 h. At 1 h before infection, culture medium was changed to fresh medium; and at the time of infection, USA300 (grown to  $OD_{600} = 0.4$ – $0.6$ ) was added at an  $\text{MOI} = 10$  to the culture medium. After 1.5 h, cells were washed  $5\times$



with PBS, followed by exposure to medium containing gentamicin 200 µg/mL. Cells were then washed 5× with sterilized PBS. After being washed with PBS, cells were stained with wheat germ agglutinin Alexa Fluor™ 555 conjugate (Invitrogen, Waltham, MA) for labeling of the cell membrane<sup>58</sup>. For examination of intracellular survival, fresh RPMI 1640 medium was added, and cells were placed in a humidified 37 °C, 5% CO<sub>2</sub> incubator for 4 and 8 h followed by the same staining procedure. All fluorescent images were taken with a Leica DMI8 fluorescence microscope (Leica Microsystems) equipped with a Leica DFC9000 GT VSC-12294 camera under HC PL APO 100× oil immersion lens. Gamma, brightness, and contrast were adjusted identically for the compared image sets using LAS X software (version 3.7.2.22383).

### Liquid chromatography mass spectrometry

**Extraction of blood metabolites.** For determination of metabolites in blank plasma, plasma was separated by centrifugation at  $845 \times g$  at 4 °C for 15 min, after which 200 µL of plasma was mixed with 400 µL of cold methanol (v/v ratio 1:2). For determination of plasma metabolites upon consumption by bacteria, bacterial culture was added to 2-mL aliquots of whole blood at an initial OD<sub>600</sub> = 0.02. The samples were incubated at 37 °C, with shaking at 150 rpm for various time points from 3 to 36 h. Whole blood to which no bacteria were added was used as the control 0 h sample. At the designated time points, whole blood samples were centrifuged for Z.

**Extraction of bacterial bacillithiol.** For determination of bacterial bacillithiol levels, USA300 was inoculated into whole blood or TSB at an OD<sub>600</sub> = 0.02 with shaking at 150 rpm at 37 °C. At 9, 12, and 24 h post-inoculation, samples were centrifuged at 4 °C,  $6010 \times g$  for 6 min for the collection of bacterial cells. Bacterial cells collected at a log phase (OD<sub>600</sub> = 0.5) were defined as a 0 h sample. The resulting pellet was quenched by the addition of quenching buffer (40:40:20; Acetonitrile:Methanol:Water). Bacterial cells were lysed by mechanical disruption using 0.1 mm glass beads and a precellys homogenizer (Bertin Technologies, Montigny-le Bretonneux, France) with 12 cycles of 10,000 rpm, 30 sec cycle. Samples were placed on ice in-between each cycle for the prevention of protein degradation. Lysates were centrifuged at 4 °C,  $15,871 \times g$  for 5 min, after which supernatant was added to Spin-X centrifuge tubes (Corning Inc.) and centrifuged at 4 °C,  $15,871 \times g$  one more time.

**Liquid chromatography mass spectrometry analysis.** Blood metabolites and bacillithiol were analyzed with time-of-flight (TOF) mass spectrometry (Agilent 6230, Santa Clara, CA) coupled with a liquid chromatography system (Agilent 1290) operated in both positive and negative modes. The mobile phase consisted of solvent A (ddH<sub>2</sub>O with 0.2% formic acid) and solvent B (acetonitrile with 0.2% formic acid). The gradient condition was as following: 0–2 min, 85% B; 3–5 min, 80% B; 6–7 min, 75% B; 8–9 min, 70% B; 10–11.1 min, 50% B; 11.1–14 min 20% B; 14.1–24 min 5% B followed by a 10 min re-equilibration period at 85% B at a flow rate of 0.4 mL/min. The abundance of extracted metabolite ion intensities was acquired using Profinder 6.0<sup>59,60</sup>. Bacillithiol levels were all normalized by the bacterial CFU measured for each sample.

### Growth curve measurement

For the measurement of growth of all mutant strains, strains (grown to OD<sub>600</sub> = 0.4–0.6) were added to TSB in 96-well plates at an initial OD<sub>600</sub> of 0.002. Growth was observed using a plate reader (BioTek, Winooski, VT) at 30 °C for 20 to 30 h.

### Measurement of bacterial minimum inhibitory concentration

To determine the concentration of oligomycin A that does not exhibit any effect on bacteria, a minimum inhibitory concentration (MIC) measurement was performed. Oligomycin A was serially diluted from 120 µM in a 96-well plate in TSB, in which USA300 was grown from

OD<sub>600</sub> = 0.002 for 24 h. The final OD<sub>600</sub> was measured by the plate reader (BioTek) for the determination of oligomycin A concentration affecting bacterial growth.

### Cell cytotoxicity

To determine the concentration of oligomycin A which does not exhibit toxicity on host A549 cells, cell cytotoxicity measurement was performed using the CytoTox-Glo™ assay (Promega, Madison, WI), according to the manufacturer's instructions<sup>61</sup>. Briefly, A549 cells were seeded in white-bottom 96-well plates at a density of  $1 \times 10^4$  cells/well. After 24 h of incubation in a 37 °C, 5% CO<sub>2</sub> incubator, cells were treated with 0–120 µM oligomycin A for 8 h, after which a substrate that luminesces upon reaction with intracellular organelles but cannot cross the intact membrane of live cells is added to measure cytotoxicity. The fluorescence intensity was measured using the Synergy HTX multi-mode plate reader (BioTek).

### Statistical analyses

Statistical analyses between experimental groups were conducted by a two-sided, unpaired Student's *t*-test using Microsoft Excel (v.16.98). The results were expressed as the mean ± SD of 3 biological replicates representative of duplicate or triplicate independent experiments. Differences between groups were inferred as significant for  $P < 0.05$ . The exact *P* values are denoted in the **Source Data** file and the figures.

### Reporting summary

Further information on research design is available in the Nature Portfolio Reporting Summary linked to this article.

### Data availability

All datasets generated during this study are available in the **Source Data** file. All the raw data generated by the Tn-seq are available in a public repository, the NCBI BioProject database, [PRJNA1236917](https://www.ncbi.nlm.nih.gov/bioproject/PRJNA1236917). The raw data generated by mass spectrometry analysis are deposited in the NIH Common Fund's National Metabolomics Data Repository (NMDR) website, the Metabolomics Workbench, <https://www.metabolomicsworkbench.org/> under the Project ID PR002520. The data can be accessed directly via its Project <https://doi.org/10.21228/M8WZ6W>. Source data are provided with this paper.

### Code availability

Codes needed for processing of the sequencing data is available from GitHub (<https://github.com/SuzanneWalkerLab/SSATnSeq>)<sup>26</sup>.

### References

- Kern, W. V. & Rieg, S. Burden of bacterial bloodstream infection—a brief update on epidemiology and significance of multidrug-resistant pathogens. *Clin. Microbiol. Infect.* **26**, 151–157 (2020).
- Tong, S. Y., Davis, J. S., Eichenberger, E., Holland, T. L. & Fowler, V. G. Jr Staphylococcus aureus infections: epidemiology, pathophysiology, clinical manifestations, and management. *Clin. Microbiol. Rev.* **28**, 603–661 (2015).
- Collaborators, G. B. D. A. R. Global mortality associated with 33 bacterial pathogens in 2019: a systematic analysis for the Global Burden of Disease Study 2019. *Lancet* **400**, 2221–2248 (2022).
- Garzoni, C. & Kelley, W. L. Staphylococcus aureus: new evidence for intracellular persistence. *Trends Microbiol.* **17**, 59–65 (2009).
- Peyrusson, F. et al. Intracellular Staphylococcus aureus persists upon antibiotic exposure. *Nat. Commun.* **11**, 2200 (2020).
- Garzoni, C. & Kelley, W. L. Return of the Trojan horse: intracellular phenotype switching and immune evasion by Staphylococcus aureus. *EMBO Mol. Med.* **3**, 115–117 (2011).
- Turner, N. A. et al. Methicillin-resistant Staphylococcus aureus: an overview of basic and clinical research. *Nat. Rev. Microbiol.* **17**, 203–218 (2019).

8. Potter, A. D. et al. Host nutrient milieu drives an essential role for aspartate biosynthesis during invasive *Staphylococcus aureus* infection. *Proc. Natl Acad. Sci. USA* **117**, 12394–12401 (2020).
9. Lowy, F. D. Is *Staphylococcus aureus* an intracellular pathogen? *Trends Microbiol.* **8**, 341–343 (2000).
10. Tiwari, N. et al. The SrrAB two-component system regulates *Staphylococcus aureus* pathogenicity through redox sensitive cysteines. *Proc. Natl Acad. Sci. USA* **117**, 10989–10999 (2020).
11. Crosby, H. A. et al. The *Staphylococcus aureus* ArlRS two-component system regulates virulence factor expression through MgrA. *Mol. Microbiol.* **113**, 103–122 (2020).
12. Novick, R. P. Autoinduction and signal transduction in the regulation of staphylococcal virulence. *Mol. Microbiol.* **48**, 1429–1449 (2003).
13. Munzenmayer, L. et al. Influence of Sae-regulated and Agr-regulated factors on the escape of *Staphylococcus aureus* from human macrophages. *Cell Microbiol.* **18**, 1172–1183 (2016).
14. Sun, F. et al. In the *Staphylococcus aureus* two-component system sae, the response regulator SaeR binds to a direct repeat sequence and DNA binding requires phosphorylation by the sensor kinase SaeS. *J. Bacteriol.* **192**, 2111–2127 (2010).
15. Mashruwala, A. A., Gries, C. M., Scherr, T. D., Kielian, T. & Boyd, J. M. SaeRS is responsive to cellular respiratory status and regulates fermentative biofilm formation in *Staphylococcus aureus*. *Infect Immun* **85** (2017).
16. Pastar, I. et al. Intracellular *Staphylococcus aureus* triggers pyroptosis and contributes to inhibition of healing due to perforin-2 suppression. *J. Clin. Invest.* **131** (2021).
17. Flannagan, R. S., Kuiack, R. C., McGavin, M. J. & Heinrichs, D. E. *Staphylococcus aureus* Uses the GraXRS regulatory system to sense and adapt to the acidified Phagolysosome in Macrophages. *mBio* **9**, e01143–18 (2018).
18. Nakaminami, H. et al. Efflux transporter of Siderophore Staphyloferrin A in *Staphylococcus aureus* contributes to bacterial fitness in abscesses and epithelial cells. *Infect. Immun.* **85**, e00358–17 (2017).
19. Edwards, A. M., Potts, J. R., Josefsson, E. & Massey, R. C. *Staphylococcus aureus* host cell invasion and virulence in sepsis is facilitated by the multiple repeats within FnBPA. *PLoS Pathog.* **6**, e1000964 (2010).
20. Strobel, M. et al. Post-invasion events after infection with *Staphylococcus aureus* are strongly dependent on both the host cell type and the infecting *S. aureus* strain. *Clin. Microbiol. Infect.* **22**, 799–809 (2016).
21. Alam, M. T. et al. Transmission and microevolution of USA300 MRSA in U.S. households: evidence from whole-genome sequencing. *mBio* **6**, e00054 (2015).
22. Tenover, F. C. & Goering, R. V. Methicillin-resistant *Staphylococcus aureus* strain USA300: origin and epidemiology. *J. Antimicrob. Chemother.* **64**, 441–446 (2009).
23. Goncheva, M. I., Gibson, R. M., Shouldice, A. C., Dikeakos, J. D. & Heinrichs, D. E. The *Staphylococcus aureus* protein IsdA increases SARS CoV-2 replication by modulating JAK-STAT signaling. *iScience* **26**, 105975 (2023).
24. Santiago, M. et al. A new platform for ultra-high density *Staphylococcus aureus* transposon libraries. *BMC Genomics* **16**, 252 (2015).
25. Liang, X. et al. Inactivation of a two-component signal transduction system, SaeRS, eliminates adherence and attenuates virulence of *Staphylococcus aureus*. *Infect. Immun.* **74**, 4655–4665 (2006).
26. Coe, K. A. et al. Multi-strain Tn-Seq reveals common daptomycin resistance determinants in *Staphylococcus aureus*. *PLoS Pathog.* **15**, e1007862 (2019).
27. Santiago, M. et al. Genome-wide mutant profiling predicts the mechanism of a Lipid II binding antibiotic. *Nat. Chem. Biol.* **14**, 601–608 (2018).
28. Liu, Q., Yeo, W. S. & Bae, T. The SaeRS Two-Component System of *Staphylococcus aureus*. *Genes* **7**, 81 (2016).
29. Hawdon, N. A. et al. Cellular responses of A549 alveolar epithelial cells to serially collected *Pseudomonas aeruginosa* from cystic fibrosis patients at different stages of pulmonary infection. *FEMS Immunol. Med. Microbiol.* **59**, 207–220 (2010).
30. Wassmann, C. S. et al. The menaquinone pathway is important for susceptibility of *Staphylococcus aureus* to the antibiotic adjuvant, cannabidiol. *Microbiol Res* **257**, 126974 (2022).
31. Lee, B. S., Singh, S. & Pethe, K. Inhibiting respiration as a novel antibiotic strategy. *Curr. Opin. Microbiol.* **74**, 102327 (2023).
32. Devenish, R. J., Prescott, M., Boyle, G. M. & Nagley, P. The oligomycin axis of mitochondrial ATP synthase: OSCP and the proton channel. *J. Bioenerg. Biomembr.* **32**, 507–515 (2000).
33. Kwiecinski, J. M. & Horswill, A. R. *Staphylococcus aureus* bloodstream infections: pathogenesis and regulatory mechanisms. *Curr. Opin. Microbiol.* **53**, 51–60 (2020).
34. Seidl, K. et al. Effect of a glucose impulse on the CcpA regulon in *Staphylococcus aureus*. *BMC Microbiol.* **9**, 95 (2009).
35. Xiao, F. et al. A new CcpA binding site plays a bidirectional role in carbon catabolism in *Bacillus licheniformis*. *iScience* **24**, 102400 (2021).
36. Psychogios, N. et al. The human serum metabolome. *PLoS One* **6**, e16957 (2011).
37. Choe, M., Park, Y. H., Lee, C. R., Kim, Y. R. & Seok, Y. J. The general PTS component HPr determines the preference for glucose over mannitol. *Sci. Rep.* **7**, 43431 (2017).
38. Beisel, C. L. & Afroz, T. Rethinking the hierarchy of sugar utilization in bacteria. *J. Bacteriol.* **198**, 374–376 (2016).
39. Gorke, B. & Stulke, J. Carbon catabolite repression in bacteria: many ways to make the most out of nutrients. *Nat. Rev. Microbiol.* **6**, 613–624 (2008).
40. de Carvalho, L. P. et al. Metabolomics of *Mycobacterium tuberculosis* reveals compartmentalized co-catabolism of carbon substrates. *Chem. Biol.* **17**, 1122–1131 (2010).
41. Borah, K. et al. Metabolic fluxes for nutritional flexibility of *Mycobacterium tuberculosis*. *Mol. Syst. Biol.* **17**, e10280 (2021).
42. Benoni, R. et al. Activation of an anti-bacterial toxin by the biosynthetic enzyme CysK: mechanism of binding, interaction specificity and competition with cysteine synthase. *Sci. Rep.* **7**, 8817 (2017).
43. Linzner, N. et al. *Staphylococcus aureus* Uses the Bacilliredoxin (BrxAB)/Bacillithiol Disulfide Reductase (YpdA) Redox pathway to defend against oxidative stress under infections. *Front Microbiol* **10**, 1355 (2019).
44. Perera, V. R., Newton, G. L. & Pogliano, K. Bacillithiol: a key protective thiol in *Staphylococcus aureus*. *Expert Rev. Anti Infect. Ther.* **13**, 1089–1107 (2015).
45. Ragle, B. E., Karginov, V. A. & Bubeck-Wardenburg, J. Prevention and treatment of *Staphylococcus aureus* pneumonia with a beta-cyclodextrin derivative. *Antimicrob. Agents Chemother.* **54**, 298–304 (2010).
46. Huo, S. et al. Overcoming Planktonic and Intracellular *Staphylococcus aureus*-associated infection with a cell-penetrating peptide-conjugated antimicrobial peptide. *ACS Infect. Dis.* **6**, 3147–3162 (2020).
47. Parker, D. & Prince, A. Immunopathogenesis of *Staphylococcus aureus* pulmonary infection. *Semin. Immunopathol.* **34**, 281–297 (2012).
48. Valentino, M. D. et al. Genes contributing to *Staphylococcus aureus* fitness in abscess- and infection-related ecologies. *mBio* **5**, e01729–01714 (2014).
49. Van Tyne, D. et al. Impact of antibiotic treatment and host innate immune pressure on enterococcal adaptation in the human bloodstream. *Sci. Transl. Med.* **11**, eaat8418 (2019).

50. Lee, W. et al. Antibiotic combinations that enable one-step, targeted mutagenesis of chromosomal genes. *ACS Infect. Dis.* **4**, 1007–1018 (2018).
51. Truong-Bolduc, Q. C. et al. Role of the Tet38 Efflux Pump in *Staphylococcus aureus* Internalization and Survival in Epithelial Cells. *Infect. Immun.* **83**, 4362–4372 (2015).
52. Yang, J., Liang, X. & Ji, Y. The mutated staphylococcal H35A alpha-toxin inhibits adhesion and invasion of *Staphylococcus aureus* and group A streptococci. *Virulence* **4**, 77–81 (2013).
53. Yang, J., Liang, X. & Ji, Y. The novel transcriptional regulator SA1804 is involved in mediating the invasion and cytotoxicity of *Staphylococcus aureus*. *Front. Microbiol.* **6**, 174 (2015).
54. Fey, P. D. et al. A genetic resource for rapid and comprehensive phenotype screening of nonessential *Staphylococcus aureus* genes. *mBio* **4**, e00537–00512 (2013).
55. Buras, J. A., Holzmann, B. & Sitkovsky, M. Animal models of sepsis: setting the stage. *Nat. Rev. Drug Discov.* **4**, 854–865 (2005).
56. Tjaden, B. A computational system for identifying operons based on RNA-seq data. *Methods* **176**, 62–70 (2020).
57. Liew, A. T. F. et al. A simple plasmid-based system that allows rapid generation of tightly controlled gene expression in *Staphylococcus aureus*. *Microbiology* **157**, 666–676 (2011).
58. Legant, W. R. et al. High-density three-dimensional localization microscopy across large volumes. *Nat. Methods* **13**, 359–365 (2016).
59. Yu, J. S. et al. Potential antimicrobial activity of galloyl-flavonoid glycosides From *Woodfordia uniflora* against Methicillin-resistant *Staphylococcus aureus*. *Front Microbiol* **12**, 784504 (2021).
60. Kim, J. H. et al. Reducing Peptidoglycan crosslinking by chemical modulator reverts beta-lactam resistance in Methicillin-Resistant *Staphylococcus aureus*. *Adv. Sci.* **11**, e2400858 (2024).
61. Kesanakurti, D., Chetty, C., Rajasekhar Maddirela, D., Gujrati, M. & Rao, J. S. Functional cooperativity by direct interaction between PAK4 and MMP-2 in the regulation of anoikis resistance, migration and invasion in glioma. *Cell Death Dis.* **3**, e445 (2012).

## Acknowledgements

We thank all members of the Wonsik Lee laboratory for their help in the experiments. We also thank the TEM analysis center of KIST for help in TEM imaging. This work was supported by the National Research Foundation (NRF) of Korea (NRF-2020M3A9H5104234, RS-2023-00228746, RS-2022-NR070873, and RS-2025-00555658 to W.L. and NRF-2020R111A1A01052803 and RS-2023-00243009 to J.C.). This work was also supported by the National Institutes of Health of the United States (P01AI083214 to S.W.). The schematics in Fig. 1a, Fig. 3a, Fig. 4a, Fig. 6a, and Fig. 6b were created using BioRender.

## Author contributions

W.L. and S.W. conceived the project. W.L., S.W., and J.C. designed and coordinated the overall study. The experiments and data analysis were performed by J.C., C.L., I.K., J.K., J.H.K., and T.Y. The manuscript was drafted by W.L., J.C., C.L., D.H., and S.W., and edited by input from all authors.

## Competing interests

The authors declare no competing interests.

## Additional information

**Supplementary information** The online version contains supplementary material available at <https://doi.org/10.1038/s41467-025-62292-x>.

**Correspondence** and requests for materials should be addressed to Suzanne Walker or Wonsik Lee.

**Peer review information** *Nature Communications* thanks the anonymous reviewers for their contribution to the peer review of this work. A peer review file is available.

**Reprints and permissions information** is available at <http://www.nature.com/reprints>

**Publisher's note** Springer Nature remains neutral with regard to jurisdictional claims in published maps and institutional affiliations.

**Open Access** This article is licensed under a Creative Commons Attribution-NonCommercial-NoDerivatives 4.0 International License, which permits any non-commercial use, sharing, distribution and reproduction in any medium or format, as long as you give appropriate credit to the original author(s) and the source, provide a link to the Creative Commons licence, and indicate if you modified the licensed material. You do not have permission under this licence to share adapted material derived from this article or parts of it. The images or other third party material in this article are included in the article's Creative Commons licence, unless indicated otherwise in a credit line to the material. If material is not included in the article's Creative Commons licence and your intended use is not permitted by statutory regulation or exceeds the permitted use, you will need to obtain permission directly from the copyright holder. To view a copy of this licence, visit <http://creativecommons.org/licenses/by-nc-nd/4.0/>.

© The Author(s) 2025